Electronic Supplementary Material (ESI) for Dalton Transactions.

Electronic Supporting Information

Capping agent dissolution method for the synthesis of metal nanosponges and their catalytic activity towards nitroarene reduction under mild conditions

*Sourav Ghosh, Balaji R. Jagirdar**

Department of Inorganic and Physical Chemistry, Indian Institute of Science, Bangalore 560012, India.

*Email address – jagirdar@iisc.ac.in

The kinetics of the catalytic reduction of 4-nitrophenol

The kinetics of the catalytic reduction of 4-nitrophenol with metal nanosponges were investigated and typical time dependent absorption spectra are shown in Fig. 8 (main manuscript). As the initial concentration of $NaBH_4$ is high as compared to 4-nitrophenol, pseudo-first order kinetics was used to compute the rate constant. Therefore, the rate equation could be expressed as

$$\frac{dc_t}{dt} = -kc_t$$

where, c is the concentration of 4-nitrophenol at time t and k is the rate constant of the reaction. Integrating the rate equation at boundary condition of: at t = 0, $^{c_t} = {}^{c_0}$ and t = t, $^{c_t} = {}^{c_t}$, results in

$$\ln\frac{c_t}{c_0} = -kt$$

Considering that absorbance of 4-nitrophenol (λ = 400 nm) is proportional to its concentration during the course of the reaction, concentration could be substituted by absorbance value. At time zero, t = 0, $^{A_0} = {}^{c_0}$ and at t = t, $^{A_t} = {}^{c_t}$, yields

$$\ln\frac{A_t}{A_0} = -kt$$

From a linear plot of $\ln(A_t/A_0)$ vs time (t), the slope gives the apparent rate constant of the reaction (Figure S11). The rate constants were calculated from the liner plots.

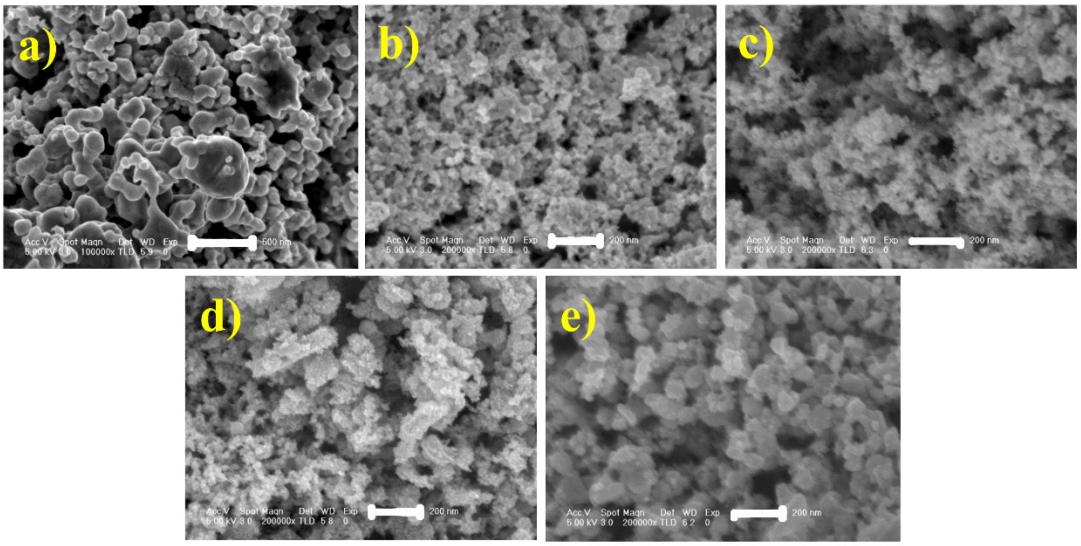

Figure S1: High resolution SEM images of a) Ag, b) Au, c) Pd, d) Pt, and e) Cu nanosponges.

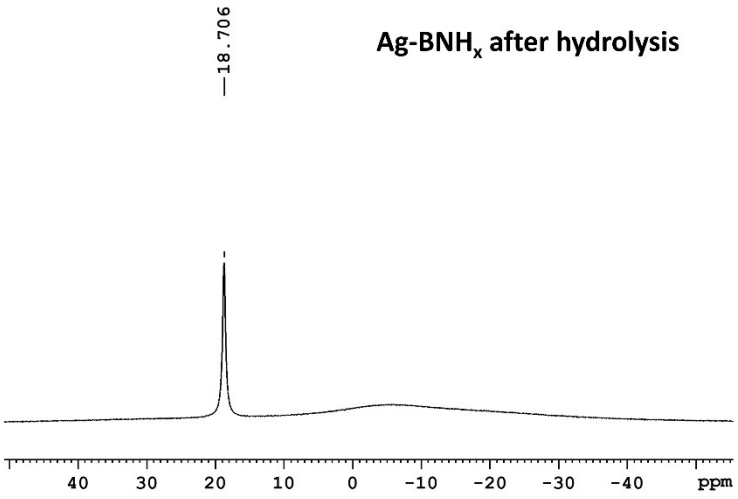

Figure S2. ^{11}B-NMR spectrum of dried filtrate obtained after the hydrolysis reaction of Ag@BNH$_x$ nanocomposite. Dried filtrates were dissolved in distil water and NMR spectra was recorded.

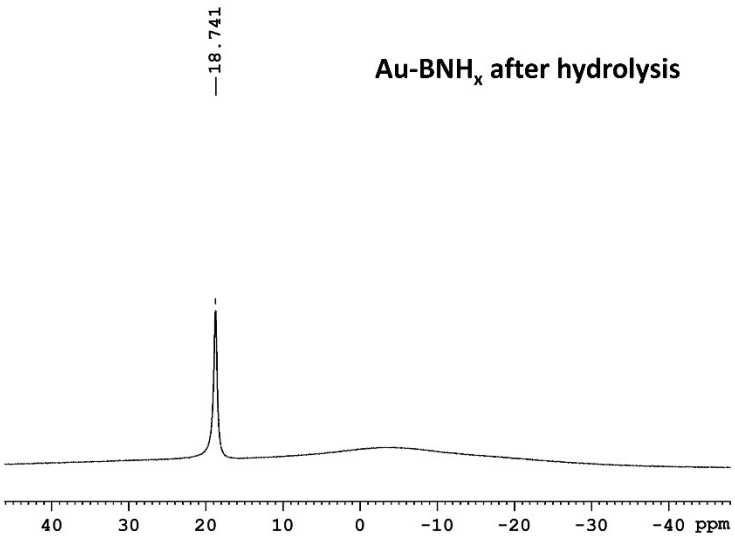

Figure S3. ^{11}B-NMR spectrum of dried filtrate obtained after the hydrolysis reaction of Au@BNH_x nanocomposite. Dried filtrate was dissolved in distil water and NMR spectra was recorded.

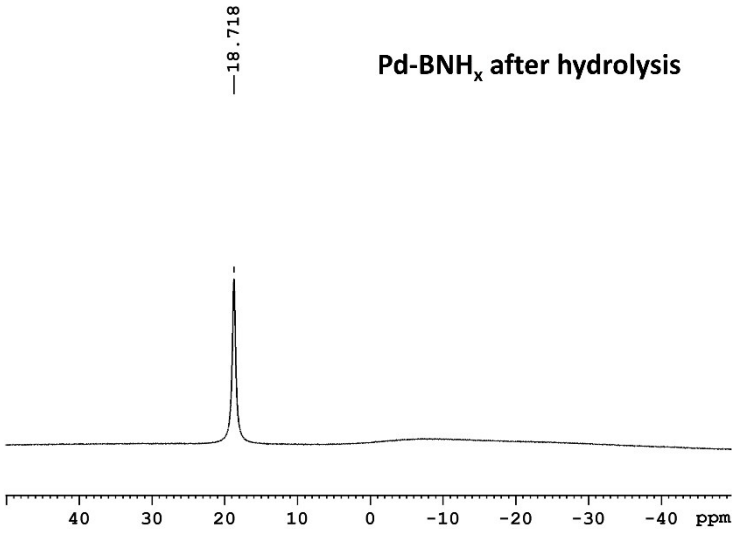

Figure S4. ^{11}B-NMR spectrum of dried filtrate obtained after the hydrolysis reaction of Pd@BNH_x nanocomposite. Dried filtrate was dissolved in distil water and NMR spectra was recorded.

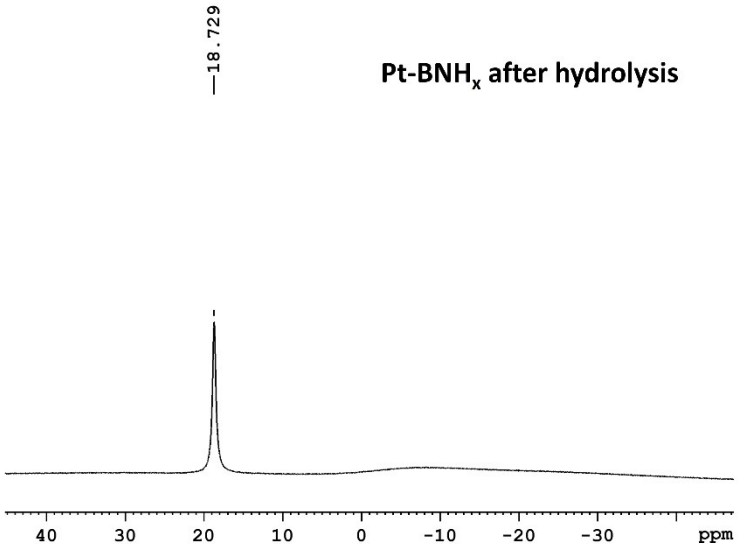

Figure S5. ^{11}B-NMR spectrum of dried filtrate obtained after the hydrolysis reaction of Pt@BNH_x nanocomposite. Dried filtrate was dissolved in distil water and NMR spectra was recorded.

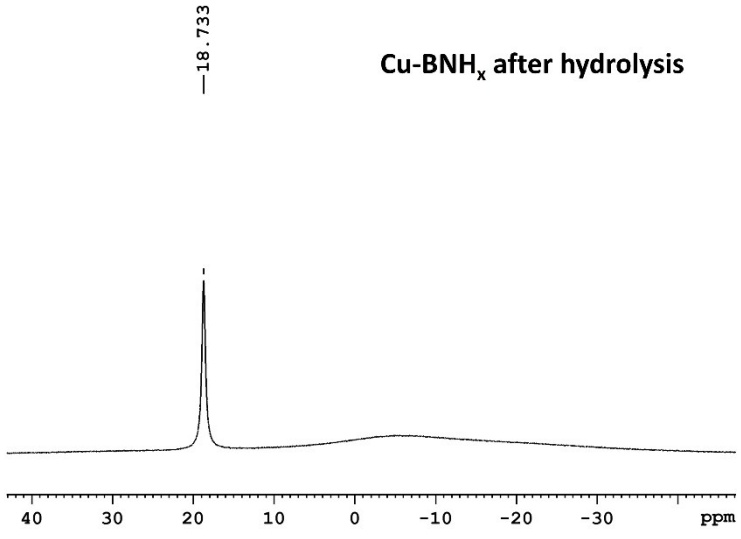

Figure S6. ^{11}B-NMR spectrum of dried filtrate obtained after the hydrolysis reaction of Cu@BNH_x nanocomposite. Dried filtrate was dissolved in distil water and NMR spectra was recorded.

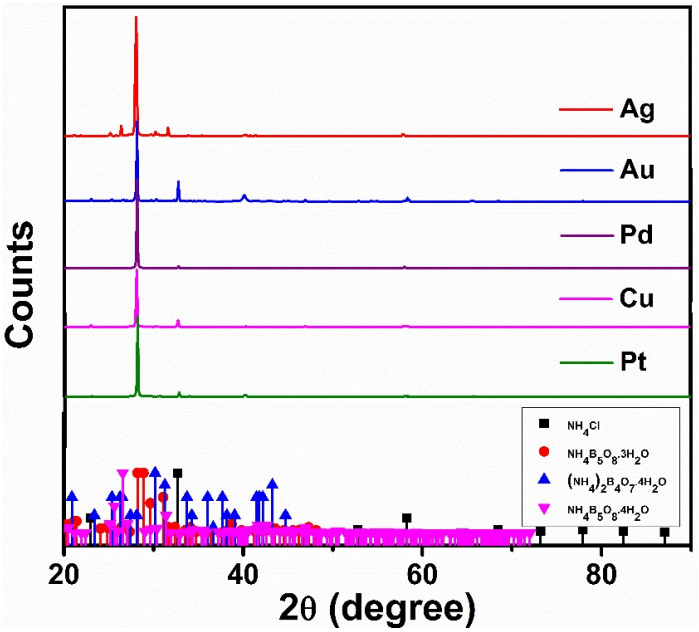

Figure S7. Powder X-ray diffraction stack plot of dried filtrates obtained after the hydrolysis reaction of different M@BNH_x (M= Ag, Au, Pd, Pt, Cu) nanocomposites. The JCPDS card number for the corresponding phases are: NH_4Cl: 07-0007; $(NH_4)_2B_4O_7.4H_2O$: 19-0061; $NH_4B_5O_8.4H_2O$: 74-1233; $NH_4B_5O_8.3H_2O$: 12-0637.

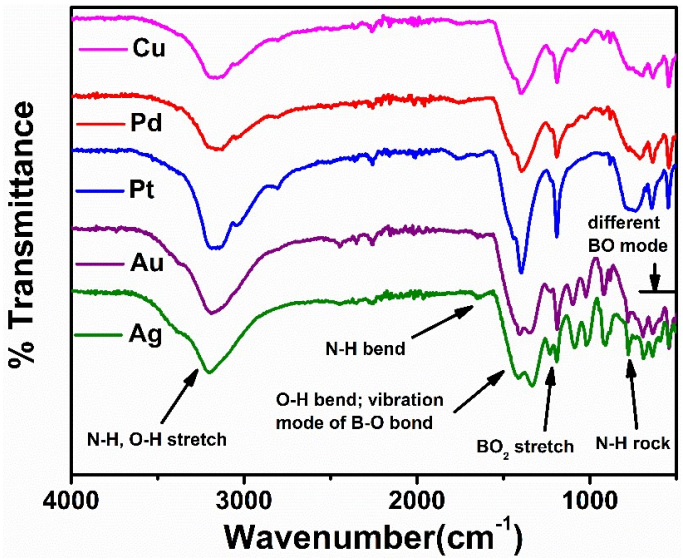

Figure S8. FT-IR spectral stack plot of dried filtrates obtained after the hydrolysis reaction of M@BNH_x (M= Ag, Au, Pd, Pt, Cu) nanocomposites.

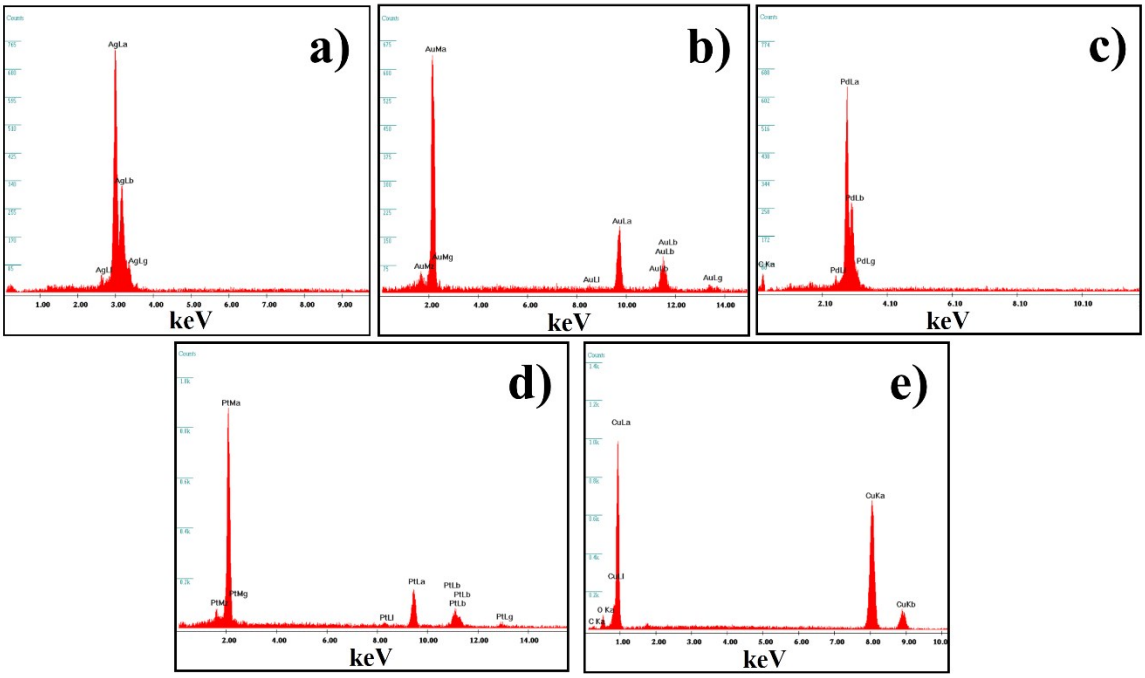

Figure S9: EDS spectra of a) Ag, b) Au, c) Pd, d) Pt, and e) Cu nanosponges.

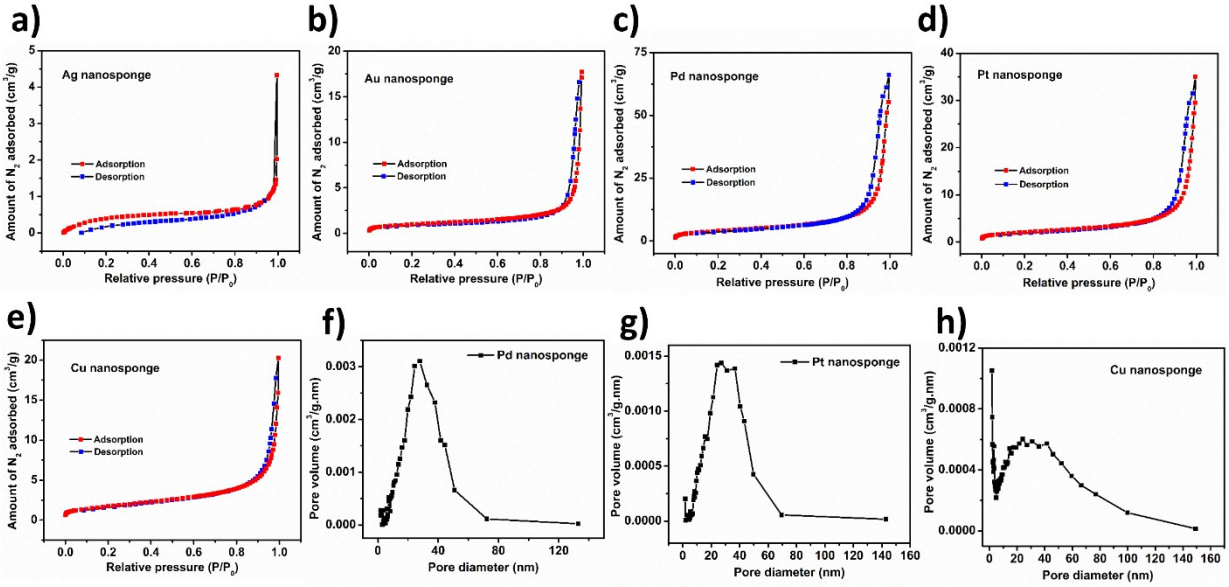

Figure S10: BET surface area of a) Ag, b) Au, c) Pd, d) Pt and e) Cu nanosponges; and BJH pore size distribution (from desorption branch) of f) Pd, g) Pt and h) Cu nanosponges.

Hydrolysis of Pd@BNH$_x$ nanocomposite at different temperature

In order to evaluate the kinetics of hydrogen evolution at a different temperature, the nanocomposite of Pd@BNH$_x$ was prepared at 1:10 ratio of palladium chloride to AB. In a typical synthesis of Pd@BNH$_x$ nanocomposite, palladium chloride (89 mg, 0.5 mmol) was added in a batch-wise manner into pre-heated (60 ^{o}C) AB (155 mg, 5 mmol) in the solid state under vigorous stirring in an inert atmosphere. After completing the addition process, the mixture was allowed to stir for 3 h at 60 ^{o}C.

a) Then the reaction mixture was cooled down to room temperature (30 ^{o}C) and 10 mL of water was added subsequently. Upon addition of water, vigorous effervescence of hydrogen gas bubbles was noted. The evolved hydrogen gas was measured using a gas burette connected to the Schlenk tube. The final volume was noted by adjusting the water levels in the gas burette and the reservoir.

b) In a different reaction, after stirring for 3 h at 60 ^{o}C, 10 mL of water was added into the reaction mixture at 60 ^{o}C and the gas evolved was measured using a gas burette connected to the Schlenk tube.

After the hydrolysis, the black precipitate formed was filtered off and washed thoroughly with water several times and finally with acetone and dried over 12 h. BET surface area was measured for both the samples.

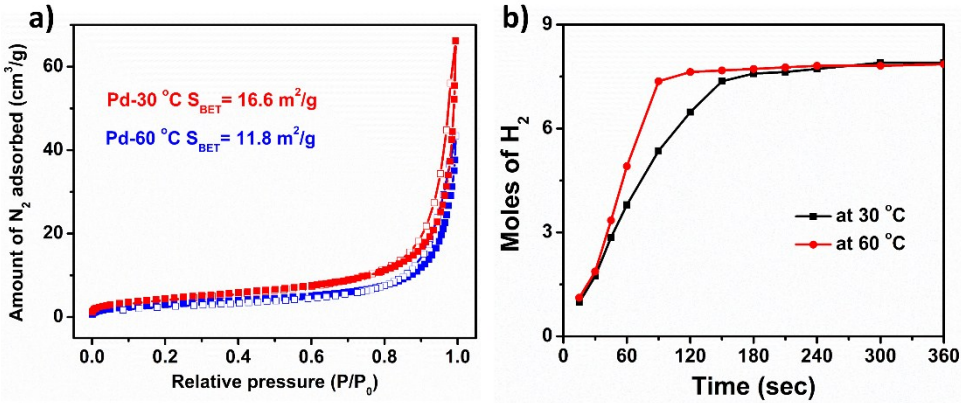

Figure S11. a) BET surface area co-plot of palladium nanosponges obtained after hydrolysis at 30 ^{o}C (red) and 60 ^{o}C (blue), solid square for adsorption branch and empty square for desorption branch; b) hydrogen generation from hydrolysis of Pd@BNH$_x$ nanocomposite.

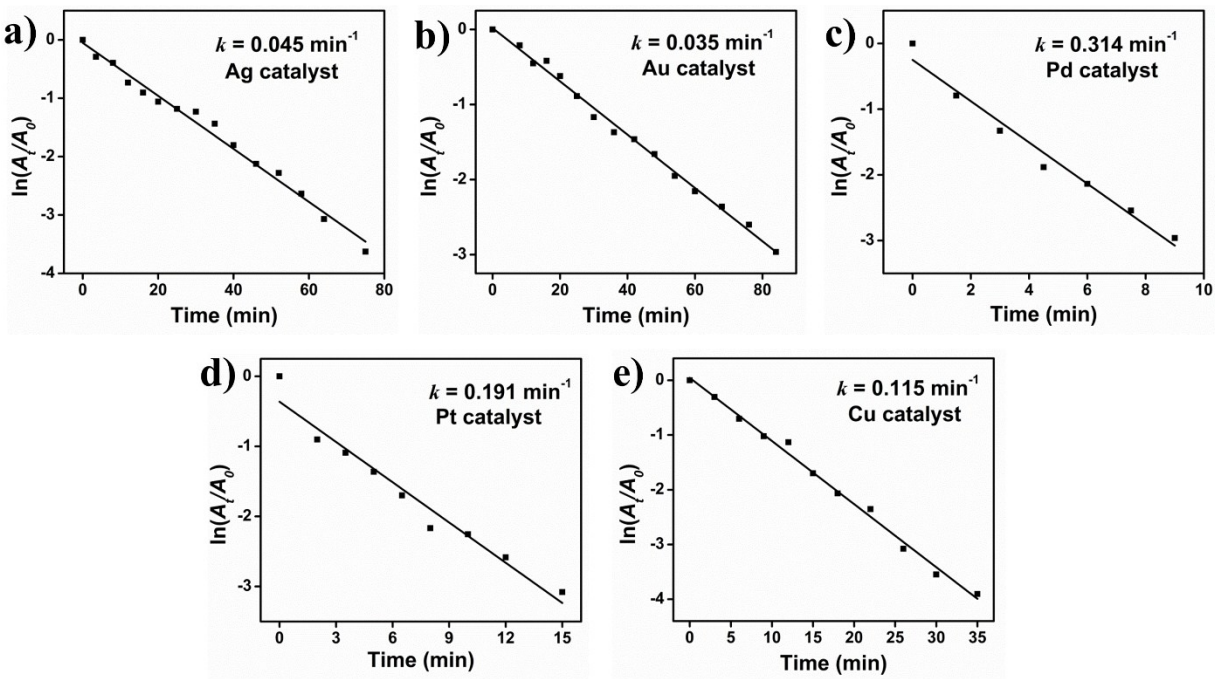

Figure S12. Kinetics analysis of the catalytic activities of metal nanosponges for the reduction of 4-nitrophenol by $NaBH_4$. Plot of $\ln(A_t/A_0)$ vs time; a) Ag, b) Au , c) Pd , d) Pt, and e) Cu nanosponges as catalysts.

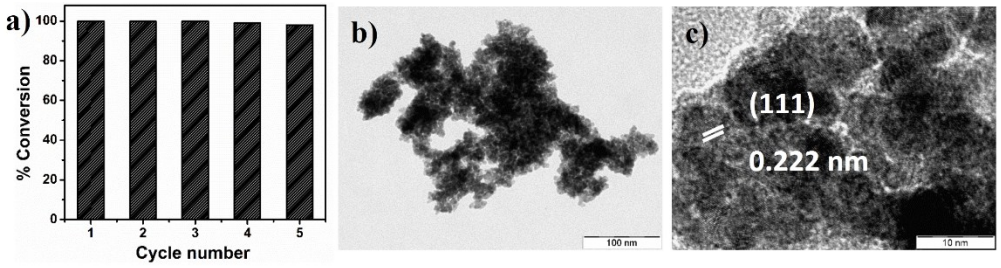

Figure S13. a) Recyclability test for the palladium nanosponge as a catalyst for nitrobenzene reduction, b) BF-TEM image and c) HRTEM image of the palladium catalyst after 5th cycle.

Table S1. Hydrogenation of nitrobenzene by palladium nanosponge using different reducing agents

Entry	Reducing agent	Time (min)	%Conv.[a]	TOF (min^{-1})[b]
1	Ammonia borane ($NH_3 \cdot BH_3$)	30	>99	33.3
2	Sodium borohydride ($NaBH_4$)	30	>99	33.3
3	Hydrazine ($N_2H_4.H_2O$)	30	6.9	2.3
4	Ammonium formate ($HCOONH_4$)	30	3.4	1.1
5	Hydrogen (H_2, 1 atm)	30	2.5	0.8

Reaction conditions: 5 mmol of nitrobenzene, 0.005 mmol of Pd nanosponge catalyst, 15 mmol of reducing agent, at constant temperature of 30 °C in 10 mL of methanol; [a]conversion to aniline was determined by GC/MS analysis using n-decane as an internal standard, [b]turnover frequency = mol (aniline)/mol (Pd nanosponge)·min.

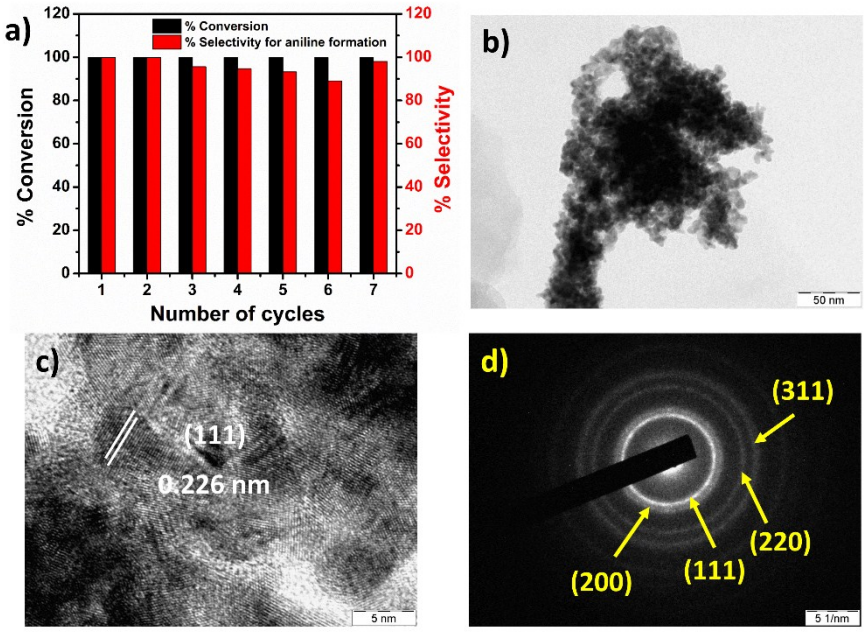

Figure S14. a) Recyclability test for the palladium nanosponge as a catalyst for nitrobenzene reduction, b) BF-TEM image, c) HRTEM image, and d) SAED pattern of the palladium catalyst after 7th cycle.

Table S2. Hydrogenation of nitrobenzene to aniline using different catalysts and reaction condition

Catalyst	Reaction conditions	Time	%Conv.	Ref.
Raney Nickel (85 mol%)	Nitrobenzene (2 mmol), NaOH (5 mmol), glycerol (3 ml) and 70 ^{o}C	5 h	11	1
Pd/C (5 mol%)	Nitrobenzene (5 mmol), 1,4-cyclohexadiene (30 mmol), methanol (10 ml), microwave and 120 ^{o}C	5 min	>99	2
Au/TiO_2 (0.8 mol%)	Nitrobenzene (0.6 mmol), N_2H_4 (2.4 mmol), 2 mL of ethanol and 60 ^{o}C	6 h	92	3
10% Pd/C	Nitrobenzene (0.28 mmol), $B_{10}H_{14}$ (10 mg), methanol (5 ml), AcOH (two drops) and heat	1.5 h	90	4
Au-MgO (0.5 mol%)	Nitrobenzene (1.08 mmol), H_2O (10 mL), $NaBH_4$ (0.05 mol), room temperature	1 h	98	5
Pd-Fe_3O_4 (1 mol%)	0.5 mmol of nitrobenzene, 1.5 mmol of NH_3BH_3, 5 mL of methanol, room temperature	5 min	68	6
Pt-Fe_3O_4 (1 mol%)	0.5 mmol of nitrobenzene, 1.5 mmol of NH_3BH_3, 5 mL of methanol, room temperature	5 min	69	6
PVP-Pd NPs (0.1 mol%)	0.25 mmol of nitrobenzne, 1 mmol of $NaBH_4$, a mixture of EtOH : H_2O 1 : 6 (final volume 3.5 mL), room temperature	1 h	97	7
Pd NPs (6 mol%)	Nitrobenzene (0.5 mmol), $(CH_3)_2NH{\cdot}BH_3$ (1.5 mmol), 3 mL of water/methanol (v/v = 2/1), room temperature	10 min	>99	8
Pd-Pol (1.7 mol%)	1.0 mmol of nitrobenzene, 10 mmol of $NaBH_4$, 5 mL of water were stirred at room temperature under nitrogen	2 h	96	9
Pd/Fe_3O_4@C (40 mg)	Nitrobenzene (1 mmol), EtOH (6 ml), $NaBH_4$ (3 mmol), at 60 ^{o}C	1 h	>99	10
Pd nanosponge (0.1 mol%)	5 mmol of nitrobenzene, 15 mmol of NH_3BH_3, 10 mL of methanol, room temperature	30 min	>99	This work

Gas chromatogram:

Reduction of nitrobenzene without catalyst

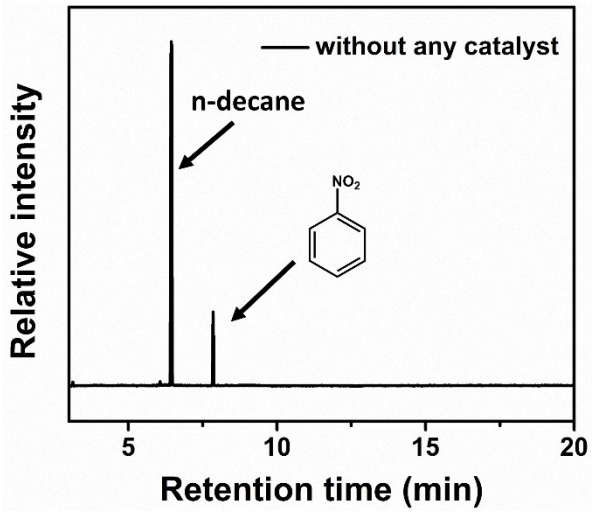

GC: Table 4 entry 1

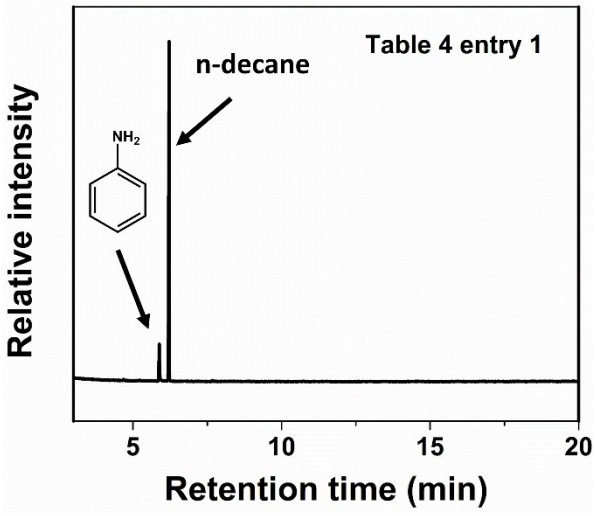

GC: Table 4 entry 2

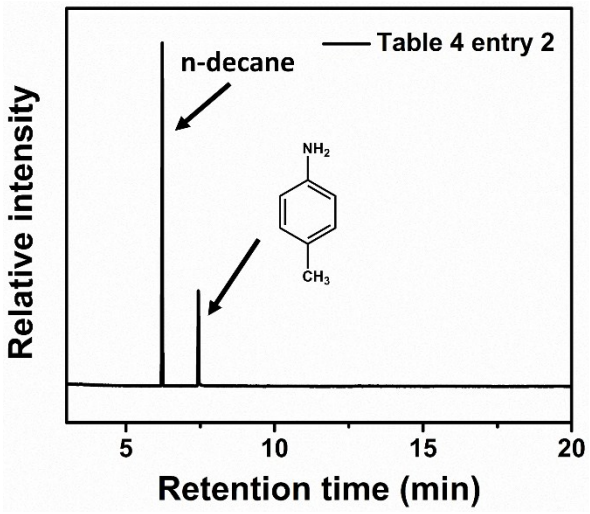

GC: Table 4 entry 3

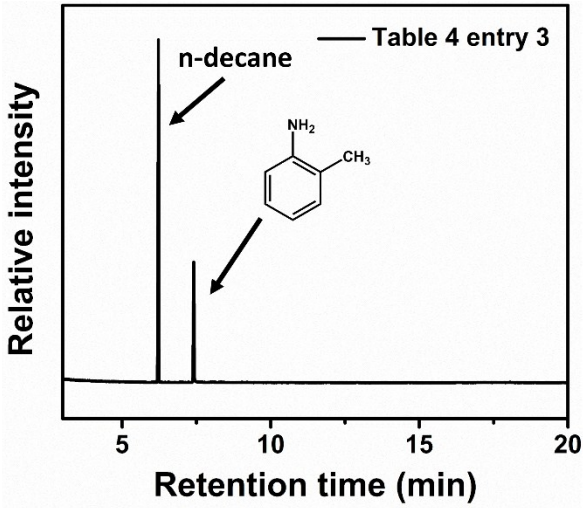

GC: Table 4 entry 4

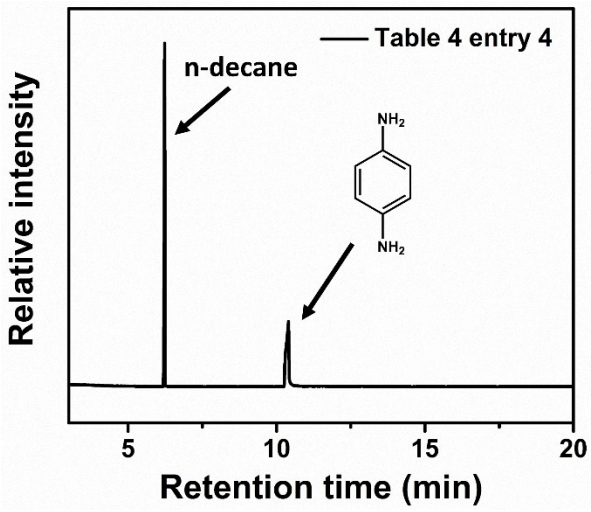

GC: Table 4 entry 5

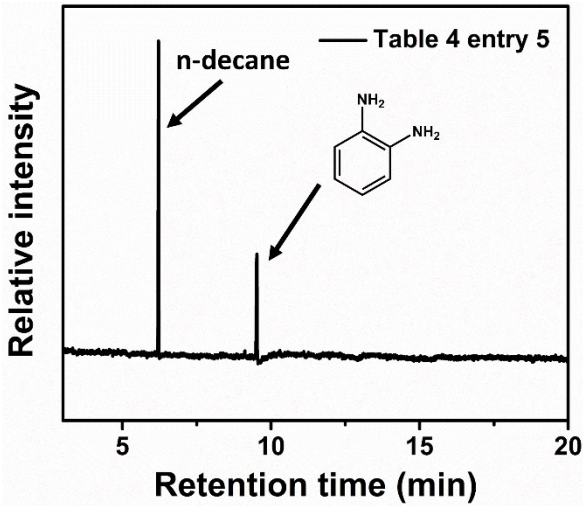

GC: Table 4 entry 6

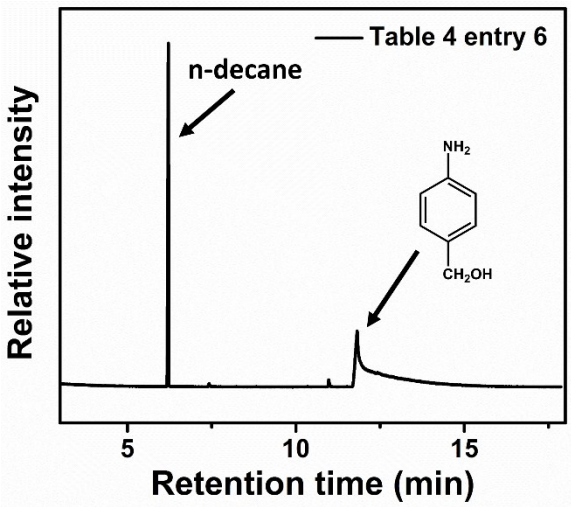

GC: Table 4 entry 7

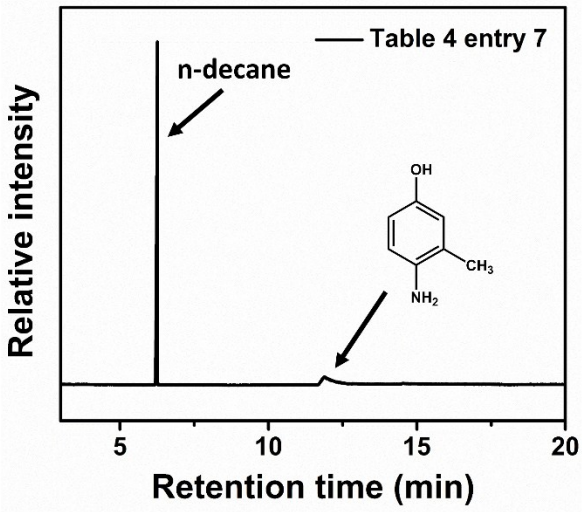

GC: Table 4 entry 8

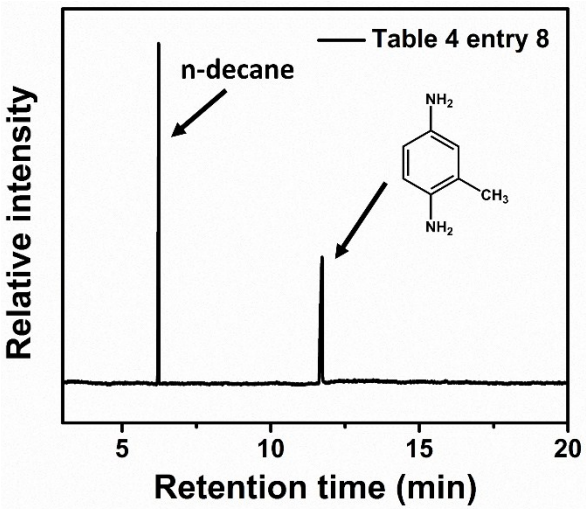

GC: Table 4 entry 9

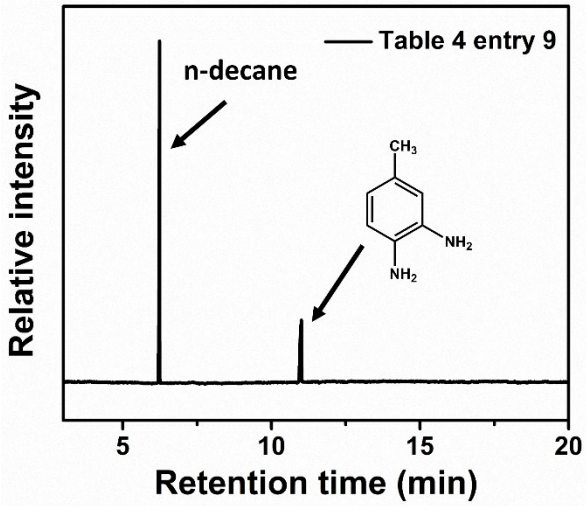

GC: Table 4 entry 10

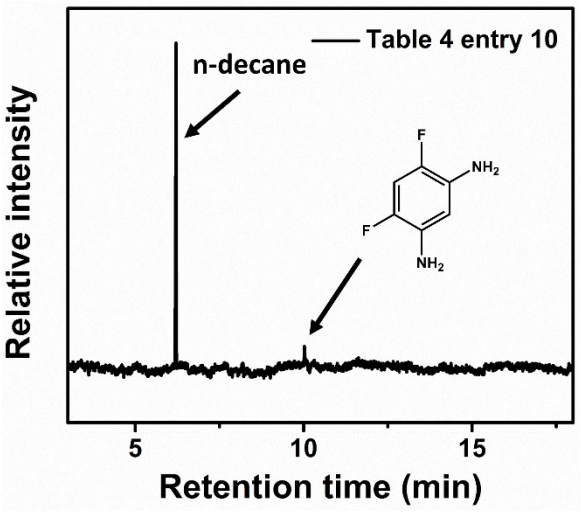

GC: Table 4 entry 11

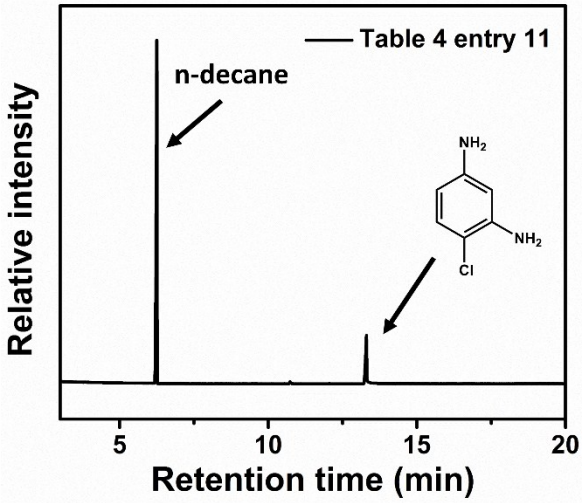

GC: Table 4 entry 12

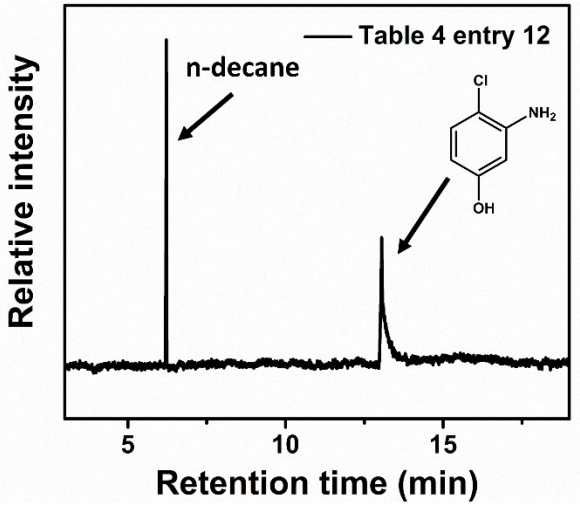

GC: Table 4 entry 13

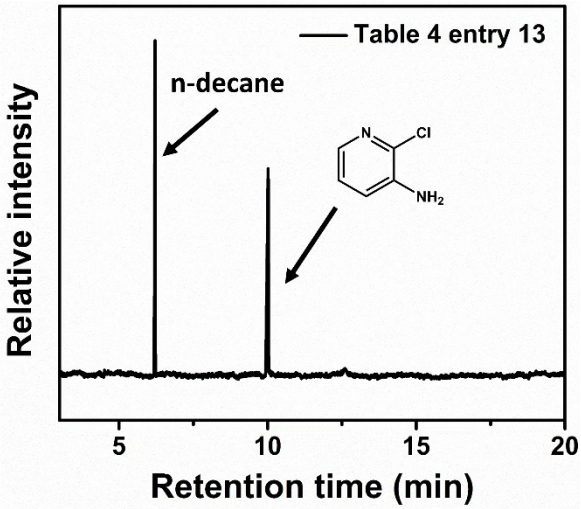

GC: Table 4 entry 14

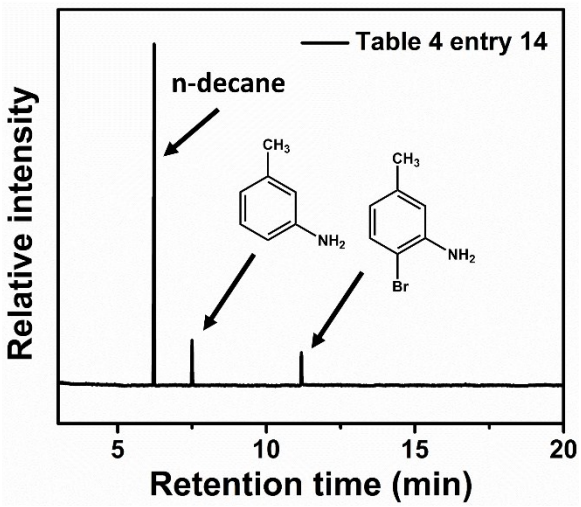

GC: Table 4 entry 15

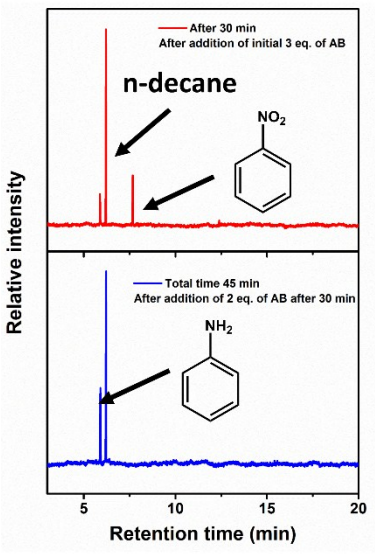

GC: Table 4 entry 16

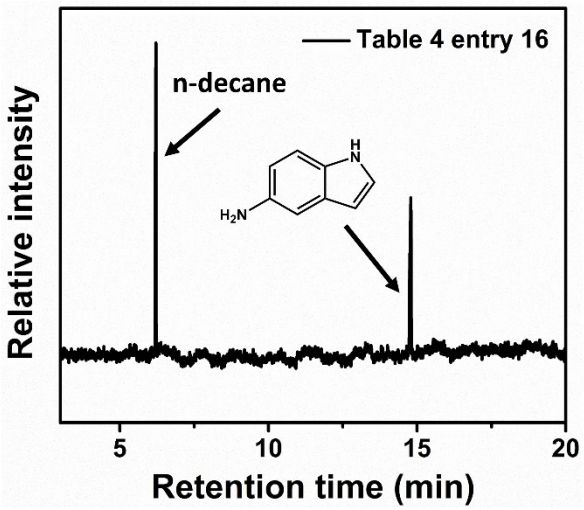

GC: Table 4 entry 17

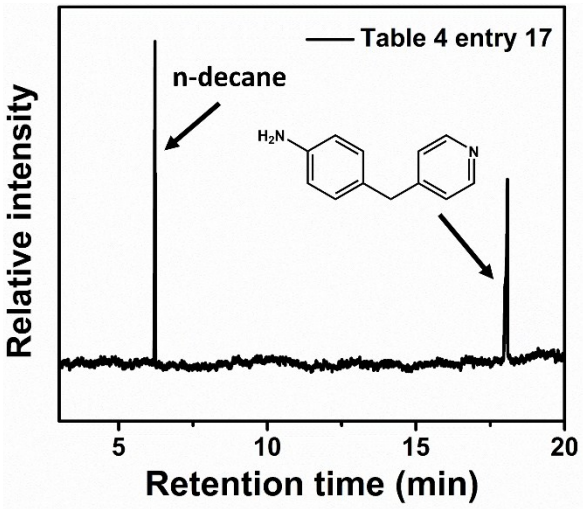

GC: Table 4 entry 18

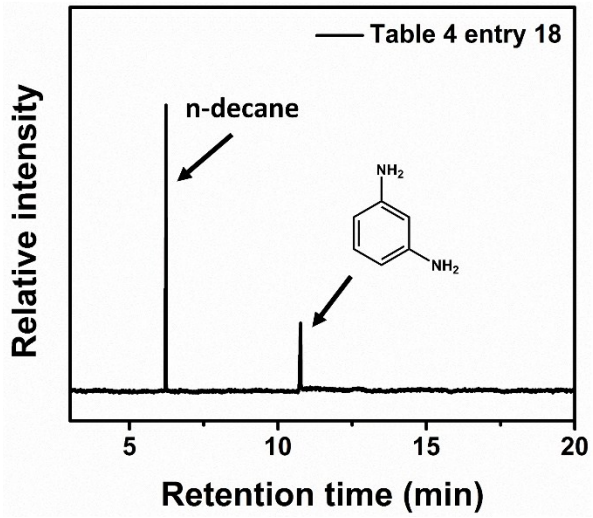

GC: Table 4 entry 19

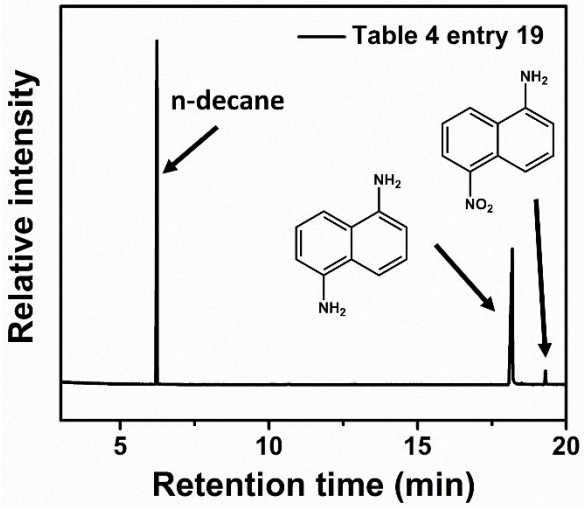

GC: Table 4 entry 20

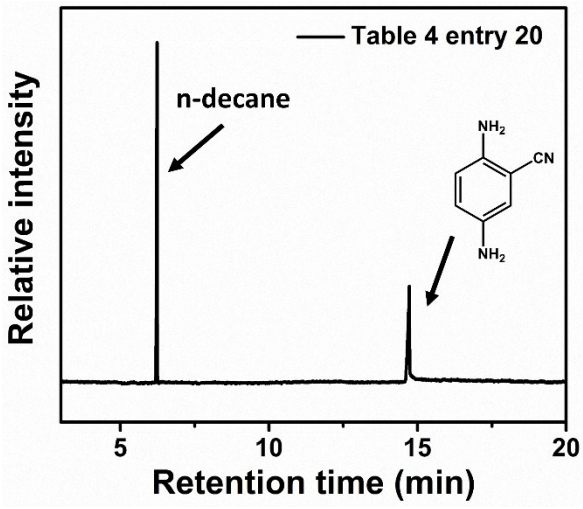

GC: Table 4 entry 21

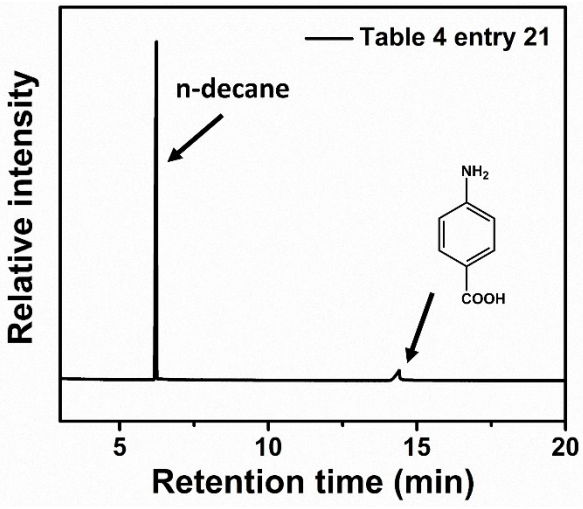

GC: Table 4 entry 22

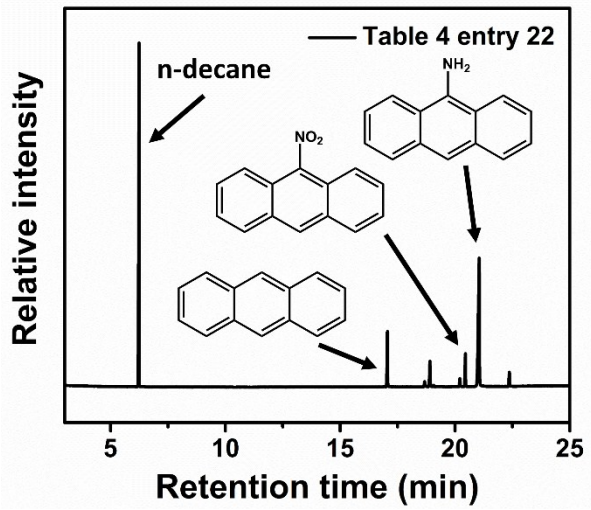

References:

1. A. Wolfson, C. Dlugy, Y. Shotland and D. Tavor, *Tetrahedron Lett.,* 2009, **50**, 5951-5953.

2. J. F. Quinn, C. E. Bryant, K. C. Golden and B. T. Gregg, *Tetrahedron Lett.*, 2010, **51**, 786-789.

3. P. L. Gkizis, M. Stratakis and I. N. Lykakis, *Catal. Commun.*, 2013, **36**, 48-51.

4. J. W. Bae, Y. J. Cho, S. H. Lee and C. M. Yoon, *Tetrahedron Lett.*, 2000, **41**, 175-177.

5. K. Layek, M. L. Kantam, M. Shirai, D. Nishio-Hamane, T. Sasaki and H. Maheswaran, *Green Chem.*, 2012, **14**, 3164-3174.

6. S. Byun, Y. Song and B. M. Kim, *ACS Appl. Mater. Interfaces*, 2016, **8**, 14637−14647.

7. P. M. Uberman, C. S. García, J. R. Rodríguez and S. E. Martín, *Green Chem.,* 2017, **19**, 739–748.

8. N. M. Patil, M. A. Bhosale and B. M. Bhanage, *RSC Adv.*, 2015, **5**, 86529–86535.

9. M. M. Dell'Anna, S. Intini, G. Romanazzi, A. Rizzuti, C. Leonelli, F. Piccinni and P. Mastrorilli, *J. Mol. Catal. A: Chem.*, 2014, **395**, 307–314.

10. N. Mei and B. Liu, *Int. J. Hydrogen Energy,* 2016, **41**, 17960-17966.